Q value of the superallowed decay of ^{22}Mg and the calibration of the ^{21}Na(p, γ) experiment

G. Savard,[1,2] J. A. Clark,[3,1] F. Buchinger,[4] J. E. Crawford,[4] S. Gulick,[4] J. C. Hardy,[5] A. A. Hecht,[1,6] V. E. Iacob,[5] J. K. P. Lee,[4] A. F. Levand,[1] B. F. Lundgren,[1] N. D. Scielzo,[1] K. S. Sharma,[3] I. Tanihata,[1] I. S. Towner,[7] W. Trimble,[1] J. C. Wang,[3,1] Y. Wang,[3] and Z. Zhou[1]

[1]*Physics Division, Argonne National Laboratory, Argonne, Illinois 60439, USA*
[2]*Department of Physics, University of Chicago, Chicago, Illinois 60637, USA*
[3]*Department of Physics and Astronomy, University of Manitoba, Winnipeg, Manitoba R3T 2N2, Canada*
[4]*Department of Physics, McGill University, Montreal, Quebec H3A 2T8, Canada*
[5]*Cyclotron Institute, Texas A&M University, College Station, Texas 77843, USA*
[6]*Department of Chemistry, University of Maryland, College Park, Maryland 20742, USA*
[7]*Department of Physics, Queen's University, Kingston, Ontario K7L 3N6, Canada*

The masses of the radioactive nuclei ^{22}Mg and ^{22}Na have been measured with the Canadian Penning trap on-line mass spectrometer to a precision of 3×10^{-8} and 1×10^{-8}, respectively. A Q_{EC} value of 4124.39(73) keV for the superallowed β decay of ^{22}Mg is obtained from the difference of these two masses. With this precise Q value, the $\mathcal{F}t$ value for this decay is determined with improved precision and is found to be consistent with the existing precision data set of superallowed Fermi emitters. This provides an important test of the isospin symmetry-breaking corrections. If the mass of ^{22}Mg determined here is used in the calibration of a recent ^{21}Na$(p, \gamma)^{22}$Mg measurement, part of the discrepancy observed in that measurement is removed.

Superallowed $0^+ \rightarrow 0^+$ decays play a key role in a number of tests of the electroweak theory. Angular momentum conservation forces these decays to be of a pure vector (Fermi decay) character. The fact that they occur between isobaric analog states, members of the same $T=1$ isospin multiplet, means that the nuclear transition matrix element is almost independent of nuclear structure: with perfect isospin symmetry, it would simply be given by a Clebsh-Gordan coefficient. In reality, it exhibits some effects of isospin symmetry breaking but only at the percent level, the same level at which the radiative corrections contribute to the transition. The ft value for such a decay, obtained from measurements of the lifetime, Q value, and branching ratio, can be corrected for these small effects to yield an $\mathcal{F}t$ value, which has the simple form [1]

$$\mathcal{F}t \equiv ft(1 + \delta_R')(1 + \delta_{NS} - \delta_C) = \frac{K}{2G_V^2(1 + \Delta_R^V)}, \quad (1)$$

with f being the statistical rate function, t the partial half-life, G_V the weak vector coupling constant, and K is a numerical constant. The small correction terms include δ_C, the isospin symmetry-breaking correction, δ_R' and δ_{NS}, the transition-dependent parts of the radiative correction, and Δ_R^V the transition-independent part. Only δ_C and δ_{NS} depend on nuclear structure.

The conserved vector current (CVC) hypothesis states that the vector current interaction is not modified by the presence of the strongly interacting nuclear system so that exactly the same value of G_V should be obtained from each superallowed decay. The existing set of nine precisely determined transitions confirms this CVC expectation at the 3 $\times 10^{-4}$ level [1]. The resultant average value of G_V, together with the Fermi coupling constant from the pure-leptonic de-

cay of the muon, yields the most precise available value for V_{ud}, the up-down quark mixing element of the Cabibbo-Kobayashi-Maskawa (CKM) matrix. This matrix is a rotation matrix connecting the weak and mass eigenstates of the quarks and, as such, must be unitary within the standard model. Currently, the most demanding test of CKM unitarity [1,2] comes from the top-row sum,

$$V_{ud}^2 + V_{us}^2 + V_{ub}^2 = 0.9968 \pm 0.0014, \quad (2)$$

which actually violates unitarity at the 2.3 σ level. The main contributors to that unitarity test are V_{ud} and V_{us}, which contribute almost equally to the total uncertainty. (Although V_{ud} is much larger in magnitude, it is known much more precisely than V_{us}.) The third element, V_{ub}, is too small to play a role here. This discrepancy has attracted considerable attention and both V_{ud} and V_{us} are now under much scrutiny. Recent work [3] indicates that the value of V_{us} might have to be shifted to one yielding a better agreement with unitarity; if this is confirmed it would only further fuel the need for a more precise V_{ud} value.

The data on the superallowed Fermi decays used to obtain V_{ud} come from over 100 different experiments and have a high degree of consistency. They contribute less than 20% of the total uncertainty on V_{ud}. However, the small theoretical corrections that must be applied to these data, especially those that have a dependence on nuclear structure effects, are more problematic and they contribute the bulk of the uncertainty. New superallowed emitters whose calculated structure-dependent corrections cover a wider range of values than those characterizing the currently known cases are considered to provide the most useful laboratory in which to test these corrections [1]. If the new $\mathcal{F}t$ values covering a wider range of corrections still produce values of G_V consis-

tent with CVC, then one can be more confident of the less-scattered corrections used in the unitarity test so far. We report here a Q-value measurement for ^{22}Mg decay, which complements recent lifetime and branching-ratio measurements [4] to yield a precise $\mathcal{F}t$ value for its superallowed transition. This is the first new superallowed case in a region of well-understood nuclear structure and consequently is the first significant step in testing the validity of the calculated structure-dependent corrections.

The mass measurements were performed at the Canadian Penning trap (CPT) mass spectrometer located on-line at the ATLAS accelerator of Argonne National Laboratory. A detailed description of the CPT spectrometer can be found elsewhere [5,6]. The ^{22}Mg and ^{22}Na activities were created by a 3.5-MeV/nucleon beam of ^{20}Ne passing through a 7-cm-long cryogenic target of ^{3}He gas held at a pressure of 700 mbar and liquid nitrogen temperature. The gas target has 1.3-mg/cm^2-thick titanium entrance and exit windows. Reaction products recoiling out of the target are carried forward by the kinematics of the reaction. They then proceed through a focusing magnetic quadrupole triplet, a velocity filter to separate the primary beam from the reaction products, and an Enge magnetic spectrograph to make the final selection and focus them on the entrance of a gas catcher system. At that point, the species of interest forms a multi-MeV continuous beam of poor ion-optical quality quite unsuitable for efficient injection into a precision ion trap, which requires a high quality eV-energy pulsed beam. We achieve the required transformation of beam properties with a gas catcher and injection system.

At the entrance of the gas catcher system, the reaction products lose most of their energy through a thin aluminum foil that can be rotated to adjust the effective thickness and hence the energy lost by the ions. The tunable aluminium degrader is followed by a high-purity 25-cm-long helium gas cell. The radioactive ions enter this gas cell through a 1.9-mg/cm^2 Havar window, losing their remaining energy and then coming to rest in the helium gas, which is pure to the ppb level and is held at roughly 150 mbar pressure. At the final stage of their slowing-down process, the ions, which have been highly charged up to this point, recapture electrons but are unlikely to recapture the final electron since helium has a higher ionization potential than any other species and hence will not give up its electrons to slow ions. The radioactive species are therefore stopped as ions in the high-purity gas and can be manipulated by static and RF electric fields. With the assistance of these electric fields, the ions are extracted from the gas cell in roughly 10 ms as a thermal beam. The ions are then separated from the helium gas extracted with them by being channelled through RF ion guides leading to a linear RF trap, where they are accumulated. This ensemble, referred to as an RF gas catcher, has been described elsewhere [7]; it provides access to essentially any radioactive species that can be produced by fusion-evaporation reactions. The ions in the linear trap are accumulated for 300 ms and transferred in a bunch to a gas-filled Penning trap where mass-selective cooling [8] is applied. The ions are mass selected there with a resolution of 1000 before being transported to the CPT spectrometer itself.

Also present after the gas cell are ions of helium and impurities ionized in the deceleration of the radioactive ions

in the helium gas. The helium ions are easily eliminated by the RF ion guide system, but it was found that by focusing on $A=22$ this experiment incurred a particular difficulty since neon is a common impurity in even the highest purity helium gas. We found that we could not discriminate against the ^{22}Ne isotope, so this isotope saturated the system. The difficulty was overcome by the addition of a cold trap, temperature-regulated at 20–30 K, in the helium purification system to remove the neon from the helium gas being fed into the gas cell. With this modification, the mass-22 radioactive ions were collected free of other contamination. The purified radioactive ions with $A=22$ were transported in bunched mode to the CPT, where the ions were captured in a second linear RF trap and further cooled by buffer-gas collisions before being transferred via a differential pumping section to the precision Penning trap, where the mass measurements take place.

The precision Penning trap is a hyperbolic trap with gold-plated OFHC (oxygen-free high conductivity) copper electrodes located in a 6-T self-shielded superconducting magnet with high field stability. The trap is in a 10^{-10} mbar vacuum section and all material used inside the magnet is nonmagnetic, including the vacuum chamber, which is made of molybdenum. This not only avoids perturbations in the homogeneity of the magnetic field but also removes a common source of magnetic-field fluctuations connected to the temperature-dependent magnetic properties of the "nonmagnetic" stainless-steel vacuum chamber typically used.

In the Penning trap, a mass measurement is performed as a frequency scan. The ions are first loaded into the trap. Remaining contaminant ions (in this case, either mostly ^{22}Na when ^{22}Mg is being measured or the reverse) are removed from the trap by a strong mass-selective RF excitation. The ions of interest are then excited to a finite magnetron orbit by a fixed-frequency dipole RF excitation and are subjected to a quadrupolar RF field, which couples the magnetron and reduced cyclotron motion when the frequency applied corresponds to the true cyclotron frequency. The ions are subsequently ejected and allowed to drift towards a microchannel-plate detector, where a time-of-flight spectrum is recorded. The process is repeated with the injection of another bunch of ions into the trap, repetition of the ion cleaning and preparation, and quadrupolar excitation at the next frequency. This process is continued over the full cyclotron excitation-frequency interval to create a scan, and scans are repeated and summed until sufficient statistics are achieved. At the true cyclotron frequency, the ions will have their magnetron motion converted to reduced cyclotron motion and hence will have higher energy, leading to a reduced time of flight to the detector [9,10]. Frequency scans for the isotopes ^{22}Mg$^+$ and ^{22}Na$^+$ are shown in Fig. 1. For these measurements, the excitation time was 0.8 s, which yields a mass resolution of $\sim 2.5 \times 10^{-7}$. The resonance line shape (linewidth of main peak, relative amplitude and spacing of sidebands) is dependent upon the Fourier transform of the excitation pulse applied (mainly by the pulse duration). All spectra, for both the unstable isotopes shown in Fig. 1 and the stable isotopes used as a calibration, were obtained under similar excitation conditions. The line shape used to fit the resonances for all isotopes was the same and determined by an initial fitting to
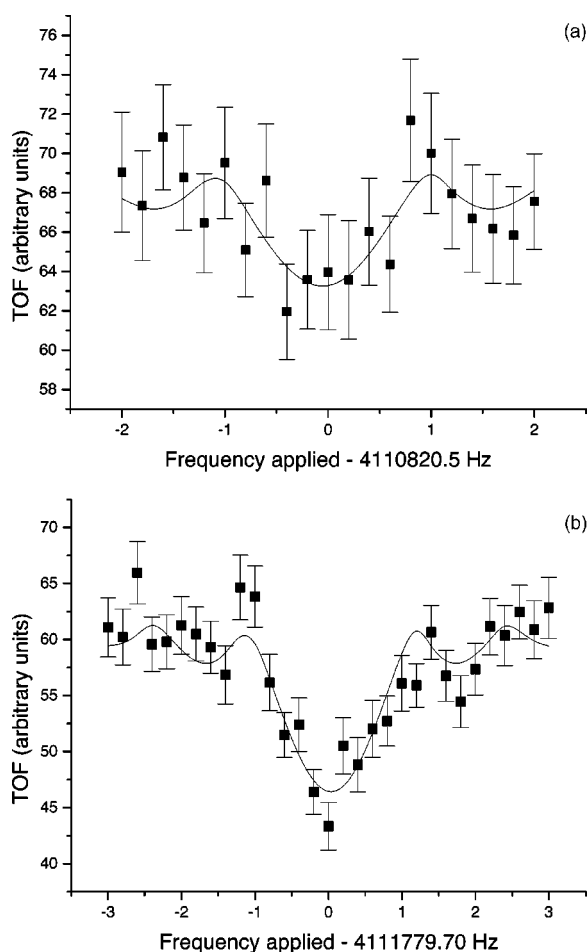
FIG. 1. A time-of-flight spectrum obtained for ^{22}Mg$^+$ (a) and ^{22}Na$^+$ (b). A quadrupole excitation of 800 ms duration was applied in both cases after we first removed the other species and established an orbital radius with a magnetron excitation. Both spectra have a full width at half maximum of ~1.1 Hz (5.5 keV), consistent with the Fourier limit. The curves shown represent the line shapes expected.
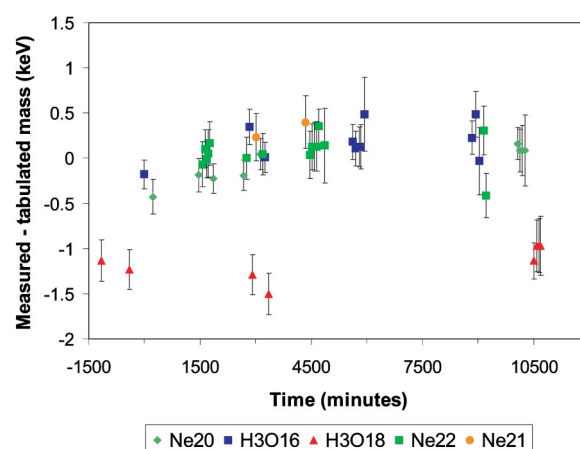

FIG. 2. (Color online) Measured mass values (plotted as the deviation from the tabulated mass values [11]) for the various isotopes versus time during the run.

the high statistics data on the calibration isotopes. After this initial determination, three parameters were allowed to vary in the individual fits: the baseline of the time-of-flight signal, the signal amplitude, and the main peak central frequency. The baseline and amplitude vary for different species because the time of flight depends on mass, and detector noise and contaminant ions introduce a flat background that is averaged with the signal from the desired species (the signal amplitude reduction is more pronounced when very few ions are detected per trap loading). The final parameter, the main peak central frequency, is the sought cyclotron frequency that yields the mass with statistical uncertainty determined by the fit. Typically the reduced χ^2 for the fits are around 1 and for the few cases where it exceeds this value the uncertainties are inflated by a factor equal to the square root of the reduced χ^2. The results of the different measurements are then averaged with the proper statistical weight to yield the final values for the cyclotron frequencies and statistical uncertainties. This procedure has been shown to provide consistent results for both high and low statistics runs.

Our experiment interleaved measurements of the mass of ^{22}Na$^+$ and ^{22}Mg$^+$ with calibrations of the magnetic field based on molecular ions of H$_2$^{18}OH$^+$ and H$_2$^{16}OH$^+$ and ions of ^{22}Ne$^+$, ^{21}Ne$^+$, and ^{20}Ne$^+$. (Measurements with neon isotopes required our bypassing the 20 K cold trap in the gas purification system.) The results from these calibration measurements, which were continued over a full week to confirm the stability of the magnetic field, are shown in Fig. 2. The important features in this figure are the precision, high reproducibility, and high stability of the measured masses, which show negligible drift within statistical accuracy over the measurement period. (No correction for field drift is applied in this figure.) The magnetic-field variation was measured to be -1.1 part in 10^{10} per hour. This shift is small at the level of accuracy required since calibration and measurements on radioactive species were interleaved in our case, but all measurements were still corrected for it.

The most insidious source of systematic errors for high-precision measurements on short-lived isotopes in a Penning trap is the possibility that the ions do not probe the same magnetic-field region. No cooling is applied in the measurement trap because of the short time available, and the spatial extent probed by the ions in the trap is determined by the ion preparation and the conditions of injection. The main factor is the timing of the capture pulse applied to let the ions into the measurement trap, which is set by the time of flight between the second linear trap, where the cooling is applied, and the measurement trap. For an electrostatic transfer system this time scales as the square root of the mass of the transferred ion, but fixed delays in the application of pulses can create small deviations from this simple scaling relation. The capture timing of all measured masses in this experiment was measured precisely and adjusted for the maximum time-of-flight signal of each species. The effectiveness of this procedure is demonstrated in Fig. 2, which shows that the masses of ^{20}Ne, ^{21}Ne, ^{22}Ne, and H$_2$^{16}OH, all known to better than 2 parts per billion, agree within the accuracy of the measurement, which is typically 1 part in 10^8. Although the data show that the use of any of these well-known isotopes is equivalent within the statistical accuracy, we have opted to be more conservative and have determined all new masses

with respect to a well-known mass with the same A value—^{22}Ne for the radioactive ions at $A=22$ and ^{21}Ne for the H$_2$^{18}OH molecule—to eliminate any unforseen mass-dependent effect. We use the 1 part per 10^8 accuracy demonstrated in the calibration (on mass ratios involving different mass number) as a conservative value for our systematic error for the new mass values obtained below on ratios of same mass number isotopes.

Measurements on the stable isotopes and molecules were performed with an average of 1.5 ions detected per cycle; the measurements on ^{22}Mg and ^{22}Na had an average of 0.35 and 0.7 ions per cycle, respectively. Shifts in cyclotron frequency due to ion-ion interactions at these low ion numbers were measured to be 2 ppb per detected ion at the CPT. Corrections to account for the lower ion number obtained with the radioactive species compared with that for the stable calibration isotopes are very small but still adjustments of 0.05 keV/c^2 and 0.04 keV/c^2 were applied to ^{22}Mg and ^{22}Na, respectively. Since all measurements on the stable isotopes are made with similar small ion numbers, no adjustments were required among them.

The mass of one of the calibrant molecular ions, H$_2$^{18}OH$^+$, is not known to very high accuracy; the uncertainty in its mass is dominated by the 0.6 keV/c^2 uncertainty in the mass of ^{18}O. We obtained a mass ratio for H$_2$^{18}OH$^+$ versus ^{21}Ne$^+$ of 1.0013712843(65). The ^{18}O mass determined from this value is found to differ by -1.5 keV/c^2 from the tabulated value [11] and yields, after a minute -0.02 keV correction for molecular binding and electronic ionization energy differences, an improved mass excess for ^{18}O of $-783.06(23)$ keV, with the quoted error containing the statistical and systematic uncertainties added in quadrature. This measurement of ^{18}O, via the molecule H$_2$^{18}OH at mass 21, is consistent with the precisely known calibrations at mass 19, 20, 21, and 22. The previous measurements that have large influence on the tabulated mass [11] of ^{18}O are inconsistent and are all less precise than the present measurement. Our measurement is compatible with the ^{18}O(^{3}He, p)^{20}F reaction result but disagrees with the mass derived from β end-point results.

For the $A=22$ radioactive species, the calibration used was ^{22}Ne$^+$ and the mass ratios observed were 1.000372238(31) and 1.000138820(11) for ^{22}Mg$^+$ versus ^{22}Ne$^+$ and ^{22}Na$^+$ versus ^{22}Ne$^+$, respectively. The final mass excesses for the two isotopes of interest, after a -0.01 keV correction for ionization energy differences, are then found

to be ΔM (^{22}Mg)$=-399.73(67)$ keV and ΔM (^{22}Na) $=-5181.12(29)$ keV. They differ by -2.7 keV and $+1.3$ keV, respectively, from the latest tabulated values [11], in both cases well outside the tabulated error bars. In the first case, our result for the mass of ^{22}Mg agrees with, but is much more precise than, the value extracted by a recent reevaluation [4] of an older measurement, $-402(3)$ keV, but is significantly higher than a recent measurement of the ^{21}Na(p, γ)^{22}Mg reaction [12], from which a mass excess of $-403.2(13)$ keV was inferred; the latter is, of course, also sensitive to the mass of ^{21}Na and the excitation energy of the state populated in that reaction, both of which now need to be remeasured. In the case of ^{22}Na, the four previous measurements used to determine the tabulated mass [11] date from 1972 or earlier and the three that disagree with our result were all derived from β-decay end-point energies.

Our new mass results yield a Q_{EC} value of 4124.39(73) keV for the superallowed decay of ^{22}Mg to the analog 0^+ state at 657.00(14)-keV excitation energy [13] in ^{22}Na. This corresponds to an f value of 418.33(44). Taking this result, together with the branching ratio, 0.5315(12), and lifetime, 3.8755(12)s, determined in reference [4] and with the appropriate correction terms [1], we obtain a corrected $\mathcal{F}t$ value of

$$\mathcal{F}t = 3081(8)\text{s}, \tag{3}$$

with the uncertainty now almost entirely due to the uncertainty of the branching ratio measurement. This value agrees with the 3072.2(8) s average $\mathcal{F}t$ value for the nine well-known cases studied so far. In itself, this result acts to support the structure-dependent corrections used in all cases to extract G_V. However, its most potent impact will have to await the $\mathcal{F}t$ value determination from complete sets of measurements of lifetimes, branching ratios and Q values of other new superallowed decays—from ^{30}S and ^{34}Ar, for example—which, together with ^{22}Mg, will span a wider range of structure-dependent corrections than has ever been covered before in a region of nuclei where the structure itself is well understood.

[1] I. S. Towner and J. C. Hardy, Phys. Rev. C **66**, 035501 (2002).

[2] S. Eidelman *et al.*, Phys. Lett. B **592**, 1 (2004).

[3] A. Sher *et al.*, Phys. Rev. Lett. **91**, 261802 (2003).

[4] J. C. Hardy *et al.*, Phys. Rev. Lett. **91**, 082501 (2003).

[5] G. Savard *et al.*, Nucl. Phys. **A626**, 353 (1997).

[6] J. Clark *et al.*, Nucl. Instrum. Methods Phys. Res. B **204**, 487 (2003).

[7] G. Savard *et al.*, Nucl. Instrum. Methods Phys. Res. B **204**, 582 (2003).

[8] G. Savard *et al.*, Phys. Lett. A **158**, 247 (1991).

[9] G. Gräff *et al.*, Z. Phys. A **297**, 35 (1980).

[10] G. Bollen *et al.*, J. Appl. Phys. **68**, 4355 (1990).

[11] G. Audi *et al.*, Nucl. Phys. **A729**, 337 (2003).

[12] S. Bishop *et al.*, Phys. Rev. Lett. **90**, 162501 (2003).

[13] P. M. Endt, Nucl. Phys. **A521**, 1 (1990).